Journal of Theoretical and Computational Chemistry
Vol. 12, No. 6 (2013) 1350054 (13 pages)

DOI: 10.1142/S0219633613500545

World Scientific
www.worldscientific.com

SEVEN-DIMENSIONAL QUANTUM DYNAMICS STUDY OF THE $H_2 + NH_2 \rightarrow H + NH_3$ REACTION ON AN INTERPOLATED POTENTIAL ENERGY SURFACE

YANG YANG*, RUI LIU*, RENZHUO WAN*,† and MINGHUI YANG*,‡

*Key Laboratory of Magnetic Resonance in Biological Systems
State Key Laboratory of Magnetic Resonance and Atomic and Molecular Physics
Wuhan Centre for Magnetic Resonance
Wuhan Institute of Physics and Mathematics
Chinese Academy of Sciences, Wuhan 430071, P. R. China

†School of Electronic and Electrical Engineering
Wuhan Textile University, Wuhan 430200, P. R. China
‡yangmh@wipm.ac.cn

Received 9 April 2013
Accepted 3 May 2013
Published 20 August 2013

Initial-state-selected time-dependent wave packet dynamics studies have been performed for the $H_2 + NH_2 \rightarrow H + NH_3$ reaction with a seven-dimensional model on a new interpolated *ab initio* potential energy surface (PES). The PES is constructed using modified Shepard interpolation Scheme and contains 1967 data points with *ab initio* calculations carried out on UCCSD(T)/aug-cc-pVTZ level. In the seven-dimensional model, NH_2 group keeps C_{2v} symmetry and two NH bonds are fixed at their equilibrium values. The total reaction probabilities are calculated when (1) the two reactants are initially at their ground states; (2) NH_2 bending mode is excited, and (3) H_2 is on its first vibrational excited state. The integral cross sections are also reported for these initial states with centrifugal-sudden approximation. Thermal rate constants are calculated for the temperature range of 200−2000 K and compared with the previous calculated values and available experimental data. Good agreements between theory and experiments for the rate constants at intermediate temperature are achieved on this PES.

Keywords: Quantum dynamics; $H_2 + NH_2$; seven-dimensional; interpolated potential energy surface; rate constant.

1. Introduction

Recently significant progress has been made toward understanding the chemical reactive dynamics involving polyatomic molecule, both experimentally and theoretically.[1−15] With the powerful computers, detailed state-to-state dynamics information could be obtained by solving nuclear Schrödinger equation.[6] However, due to the nature of quantum reactive scattering, the computational cost of the theoretical calculations is exponentially increasing with the degrees of freedom of the reaction system and it is thus difficult to perform an exact full-dimensional (FD)

calculation for the reaction beyond four-atomic system at present. For reactions including five atoms, two FD studies have been reported: One is for $H_2 + C_2H$ reaction by Wang[1] and another is for $H + NH_3$ reaction by Yang.[3] While for the $X + CH_4$ reactions, most studies are carried out with various reduced-dimensional models based on quantum scattering theory[14,16–18] although the FD study based on transition state theory has been recently presented by Manthe and co-workers.[19]

The potential energy surface (PES) plays an important role in understanding the reactive dynamics.[20,21] Nowadays PESs for three-atomic reactions have been widely used in quantum[12,22] or classical[23–28] dynamics studies, while for reactions beyond three atoms, the construction of PES is still a difficult task.[15,29–32] The combination of accurate PES and FD quantum dynamics calculations has successfully explained or predicted several important reactions, such as triatomic reaction $F + H_2$ (Ref. 33) and tetra-atomic reaction $H + H_2O$.[34] It is reasonable to extend the study to five-atomic reactions or beyond with accurate *ab initio* PES and FD quantum dynamics in the near future.

Similar to its isoelectronic reactions $H + HF$, $H + H_2O$ and $H + CH_4$, $H + NH_3 \leftrightarrow H_2 + NH_2$ is a prototype of polyatomic reaction and has drawn considerable interests recently. Zhang *et al.* have studied this reaction with a four-dimensional semi-rigid vibrating rotor target (SVRT) model[35] Yang and Corchado have studied the $H + NH_3$[36] and its reverse reaction $H_2 + NH_2$[37] with seven-dimensional models. Yang also present a FD quantum dynamics study for $H + NH_3$ reaction.[3] All these studies employed an analytic PES constructed[38] by Corchado and Espinosa-García (denoted as CE-PES hereafter) or its modification.[39] An interpolated *ab initio* PES for this reaction has been constructed by Collins and coworker (denoted as MC-PES).[40] This interpolated PES is constructed with modified Shepard interpolation scheme and contains 2000 data points which are calculated with UCCSD(T)/aug-cc-pVDZ method for both energy and derivative. In another version of MC-PES, the energy is improved with UCCSD(T)/aug-cc-pVTZ method.

In this work, we present a seven-dimensional quantum dynamics study for the $H_2 + NH_2 \rightarrow H + NH_3$ reaction on a new interpolated *ab initio* PES. The new interpolated PES utilizes the configuration of data points in MC-PES and both energy and derivative are calculated with UCCSD(T)/aug-cc-pVTZ method. With the interpolated PES, the total reaction probability and integral cross sections (ICSs) for three initial states are calculated. The thermal rate constants are also obtained and compared with the previous theoretical and experimental values. In the following of this paper, the PES will be briefly described in Sec. 2 and the quantum dynamics calculations are presented and discussed in Sec. 3. The conclusions are given in the last section.

2. Potential Energy Surface

There are two channels for H+NH_3 reaction: one is the hydrogen abstraction channel $H + NH_3 \leftrightarrow H_2 + NH_2$ reaction and another is exchange channel

$H + NH_3 \leftrightarrow NH_3 + H$. The MC-PES has been developed for both channels by an iterative procedure with classical trajectory simulations. This interpolated PES contains 2000 data points which covered all important regions of PES and its convergence has been validated.[27] This *ab initio* PES has two versions: PES1 and PES2. The PES1 is constructed with UCCSD(T)/aug-cc-pVDZ method for both energy and derivative. While for the PES2, the energy at each data points is calculated with a larger basis set aug-cc-PVTZ. These authors found that the calculations with aug-cc-pVTZ basis set would produce more accurate values for the barrier height of the exchange reaction and the well depth of NH_4 minimum.

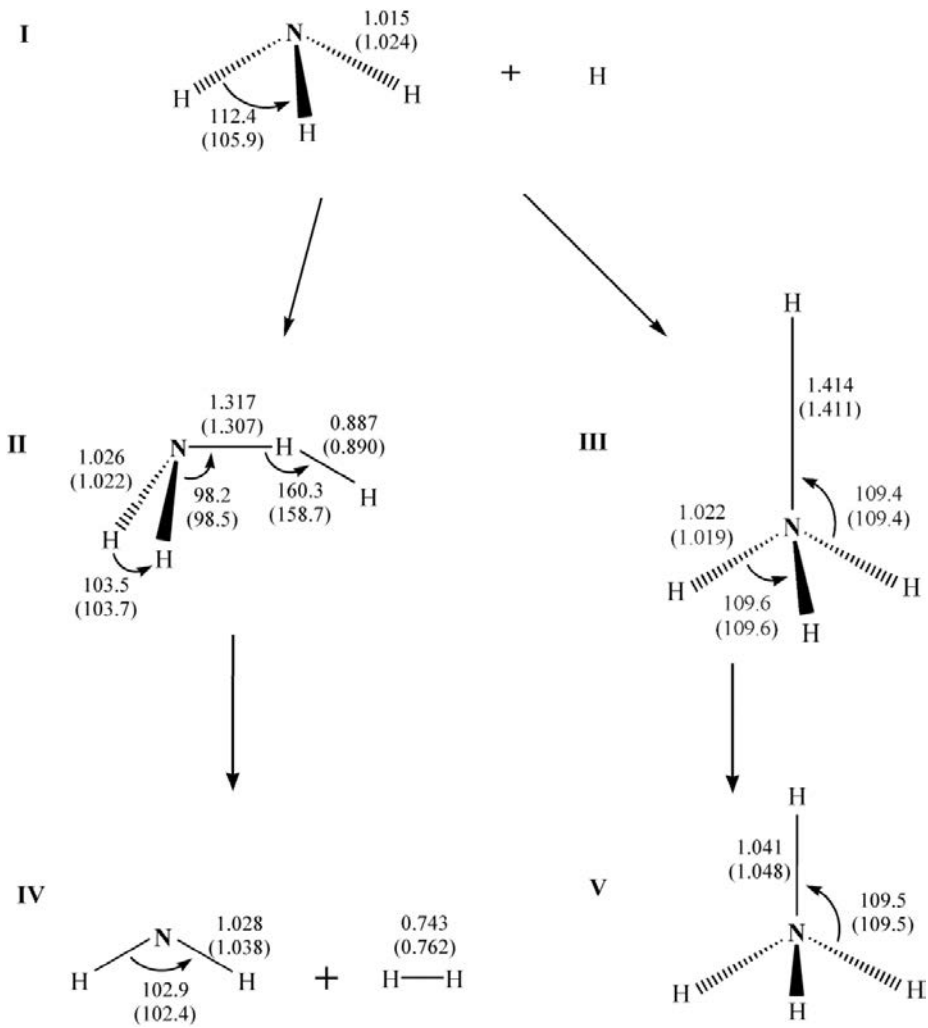

Fig. 1. The geometries of stationary points optimized with UCCSD(T)/aug-cc-pVTZ, together with the values given in Ref. 27 in parenthesis. The units of bond length and bond angle are Angstrom and Degree, respectively.

Table 1. The energy differences of the stationary points (kJ/Mol).[a]

	aug-cc-pVDZ[b]	aug-cc-pVTZ[b]	aug-cc-pVTZ[c]
$H+NH_3$ (I)	0.0	0.0	0.0
H_2+NH_2(IV)	21.0	21.3	20.77
NH_4-T_d(V)	−8.3	−10.3	−10.17
TS1-C_s(II)	62.4	61.4	61.92
TS2-C_{3v}(III)	41.9	40.2	39.69

[a]All calculation are performed with UCCSD(T) method.
[b]Ref. 27.
[c]This work.

In this work, a new interpolated *ab initio* PES is developed with both energy and derivative calculated with UCCSD(T)/aug-cc-pVTZ and utilizes the configuration of the original 2000 data points in MC-PES. A total of 1967 data points are finally included in this new PES while the other 33 data points are abandoned due to the convergence failure in *ab initio* calculations. The geometries of stationary configurations relevant to the reactions are shown in Fig. 1. The energy differences between stationary points are listed in Table 1 and are very close to the corresponding values reported in Ref. 26. In this work, all the calculations for the geometry optimization of stationary points are carried out with Gaussian 09[41] and the energy calculations for data points are carried out with MOLPRO 2012 program.[42]

3. Quantum Dynamics Calculations

3.1. *Seven-dimensional model*

The initial-state-selected wave packet (ISSWP) quantum dynamics calculation has been performed for the reverse reaction $H_2 + NH_2 \rightarrow H + NH_3$ with a seven-dimensional model. This model has been employed to study the title reaction on a modified CE-PES.[37] As ISSWP method has been widely employed in the study of reactive dynamics, only the seven-dimensional model is introduced in this paper.

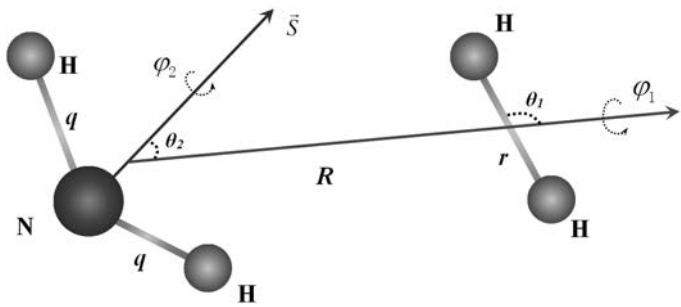

Fig. 2. Jacobi coordinates of seven-dimensional model for $H_2 + NH_2$ reaction.

In the seven-dimensional model, NH_2 keeps C_{2v} symmetry and the two NH bonds are fixed at its equilibrium positions. This approximation is reasonable because the NH bond length only changes little during the reaction as shown in Table 1 (from 1.028 Å in reactant NH_2 to 1.026 Å at saddle point). With this approximation, the Hamiltonian of the reactive system is written as:

$$\hat{H} = -\frac{1}{2\mu_R}\frac{\partial^2}{\partial R^2} - \frac{1}{2\mu_r}\frac{\partial^2}{\partial r^2} + \frac{(\hat{J}_{\text{tot}} - \hat{j}_{12})^2}{2\mu_R R^2} + \frac{\hat{j}_1^2}{2\mu_r r^2} + \hat{K}^{\text{vib}}_{NH_2} + \hat{K}^{\text{rot}}_{NH_2} + V(R, r, \chi, \theta_1, \phi_1, \theta_2, \phi_2), \quad (1)$$

here R is the distance from the center of mass (COM) of molecule NH_2 to the COM of molecule H_2; r is the bond length of H_2 molecule; χ is the H−N−H angle in NH_2 group and vector $\boldsymbol{s}$ is the C_{2v} symmetry axis of NH_2. The bending angle between R and r is defined to be θ_1; φ_1 is the azimuth angle of the rotation of H_2 around R, related to the R-s plane; θ_2 is the bending angle between R and s; and φ_2 is the azimuth angle of the rotation of NH_2 around its C_{2v} axis s. μ_R is the reduced mass of H_2−NH_2 and μ_r is the reduced mass of H_2.

In Eq. (1), the first two terms are the kinetic energy operators for R and r, respectively. $\hat{J}_{\text{tot}}$ is the total angular momentum operator of the system and $\hat{j}_{12} = \hat{j}_1 + \hat{j}_2$, where $\hat{j}_1$ and $\hat{j}_2$ are the angular momentum operators of molecules H_2 and NH_2, respectively. The third term of the Hamiltonian is the centrifugal potential and the fourth term is the rotational kinetic energy operator of molecular H_2. $\hat{K}^{\text{vib}}_{NH_2}$ and $\hat{K}^{\text{rot}}_{NH_2}$ are the vibrational and rotational kinetic operators of NH_2, respectively,[36]

$$\hat{K}^{\text{vib}}_{NH_2} = -\frac{1}{\mu_1 q^2}\frac{1}{\sin\chi}\frac{\partial}{\partial\chi}\sin\chi\frac{\partial}{\partial\chi} + \frac{1}{\mu_2 q^2}\left(\frac{\cos\chi}{\sin\chi}\frac{\partial}{\partial\chi}\sin\chi\frac{\partial}{\partial\chi} + \sin\chi\frac{\partial}{\partial\chi}\right), \quad (2)$$

$$\hat{K}^{\text{rot}}_{NH_2} = \frac{1}{2}(B_X + B_Y)\hat{j}_2^2 + \left[B_Z - \frac{1}{2}(B_X + B_Y)\right]\hat{j}_{2,z}^2 + \frac{1}{2}(B_X - B_Y)(\hat{j}_{2,+}^2 + \hat{j}_{2,-}^2), \quad (3)$$

where $\mu_1 = m_H$ and $\mu_2 = m_N m_H/(m_N + m_H)$ are the reduced masses. q is the bond length of the NH bond and is fixed at its equilibrium value of reactants. $\{B_X, B_Y, B_Z\}$ are the rotational constants and variant with the bending angle χ. $\hat{j}_{2,z}$ is the z-component of $\hat{j}_2$ and the corresponding quantum number is k_2. $\hat{j}_{2,\pm}$ are shift operators. The last term $V(R, r, \chi, \theta_1, \phi_1, \theta_2, \phi_2)$ is the potential energy.

The parity-adapted rotational basis set for the $H_2 + NH_2$ system is defined as:

$$\Phi^{J_{\text{tot}}MK\varepsilon}_{j_{12}j_1j_2k_2}(\hat{R}, \hat{r}, \hat{s}) = \sqrt{\frac{1}{2(1+\delta_{\bar{K}0}\delta_{k_20})}}\Big[\Phi^{J_{\text{tot}}MK}_{j_{12}j_1j_2k_2}(\hat{R}, \hat{r}, \hat{s}) + \varepsilon(-1)^{J_{\text{tot}}+j_{12}+j_1+j_2+k_2}\Phi^{J_{\text{tot}}M-K}_{j_{12}j_1j_2-k_2}(\hat{R}, \hat{r}, \hat{s})\Big], \quad (4)$$

here,

$$\Phi^{J_{\rm tot}MK}_{j_{12}j_1j_2k_2}(\hat{R},\hat{r},\hat{s}) = \bar{D}^{J_{\rm tot}}_{MK}(\hat{R}) Y^{j_{12}K}_{j_1j_2k_2}(\hat{r},\hat{s}) \tag{5}$$

and

$$Y^{j_{12}K}_{j_1j_2k_2}(\hat{r},\hat{s}) = \sum_m \langle j_1 m j_2 K-m | j_{12} K\rangle Y_{j_1 m}(\hat{r}) \bar{D}^{j_2}_{K-m,k_2}(\hat{s}), \tag{6}$$

with

$$Y_{j_1,m}(\hat{r}) = Y_{j_1,m}(\theta_1,\phi_1), \tag{7}$$

$$\bar{D}^{j_2}_{K-m,k_2}(\hat{s}) = \sqrt{\frac{2j_2+1}{4\pi}} D^{*j_2}_{K-m,k_2}(0,\theta_2,\phi_2), \tag{8}$$

where $\bar{K} = |K|$ and ε is the parity of wavefunction under space-inverse operation.

The time-dependent wave function is thus expanded in the parity-adapted rotational basis functions as:

$$\begin{aligned}\Psi^{J_{\rm tot}M\varepsilon} = & \sum_{n_R,n_r,n_u} \sum_{Kj_{12}j_1j_2k_2} c^{J_{\rm tot}MK\varepsilon}_{n_R n_r n_u j_{12} j_1 j_2 k_2} \\ & \times (t) G_{n_R}(R) F_{n_r}(r) H_{n_u}(\chi) \Phi^{J_{\rm tot}MK\varepsilon}_{j_{12}j_1j_2k_2}(\hat{R},\hat{r},\hat{s}),\end{aligned} \tag{9}$$

where $c^{J_{\rm tot}MK\varepsilon}_{n_R n_r n_u j_{12} j_1 j_2 k_2}(t)$ are time-dependent coefficients. n_R, n_r and n_χ are labels for the basis functions. $G_{n_R}(R)$ are sine basis functions and the basis functions $F_{n_r}(r)$ and $H_{n_u}(\chi)$ are obtained by solving one-dimensional reference Hamiltonians, defined as follows:

$$h_r(r) = -\frac{1}{2\mu_r}\frac{\partial^2}{\partial r^2} + v_r^{\rm ref}(r) \tag{10}$$

and

$$h_u(\chi) = K^{\rm vib}_{\rm NH_2} + v_u^{\rm ref}(\chi), \tag{11}$$

where $v_r^{\rm ref}(r)$ and $v_u^{\rm ref}(\chi)$ are the corresponding reference potentials.

3.2. *Calculation parameters*

In this work, L-shaped techniques were used to reduce the size of basis set.[43] A total of 96 sine basis functions are used for R ranging from 1.5 Bohr to 13.0 Bohr and 36 nodes are placed in the interaction region. About 6 and 25 basis functions for r are used in the asymptotic and interaction regions, respectively. For the NH_2 bending mode, six basis functions are used. The size of the rotational basis functions is controlled by the parameters, $j_{12} = 56$, $j_1 = 28$, $j_2 = 28$ and $k_2 = 28$. Considering parity and C_{2v} symmetry, the size of rotational basis functions is 76,000 and the number of nodes for the integration of the rotational basis set is 719,055. The size of the total basis functions is 5.75×10^8 and the number of nodes for potential energy calculation is 5.436×10^9.

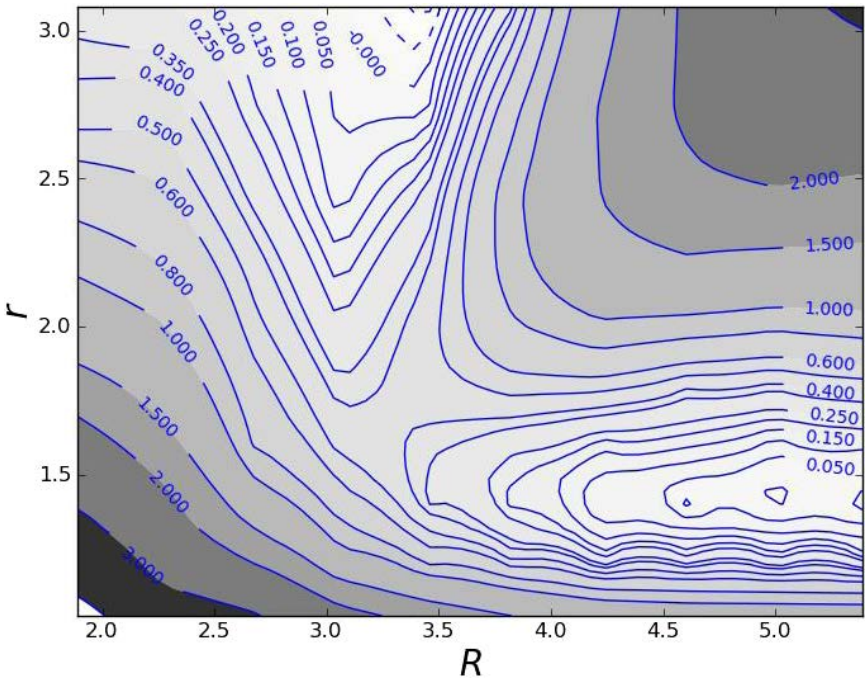

Fig. 3. Contour plot of PES (in eV) in the Jacobi coordinate (R, r). The unit of coordinates is Bohr.

3.3. *Results and discussions*

Three initial states are considered: (1) Both H_2 and NH_2 on their ground state (denoted as (0,0) state); (2) The bending mode of NH_2 is excited (denoted as (0,1) state), and (3) H_2 on its first vibrational excited state (denoted as (1,0) state). For the H_2 molecule, the zero point energy is 2171.2 cm^{-1} and the energy of the first excited state is 6323.8 cm^{-1}, corresponding to transition frequencies of 4206 cm^{-1} (0.522 eV). In this seven-dimensional model, only the bending mode of NH_2 is considered when the excitation energy is 1530.1 cm^{-1} (0.188 eV).

Figures 4(a) and 4(b) show the total reaction probabilities as a function of translational energy and total energy for three initial states, together with the probabilities calculated on CE-PES. For the ground state, the reaction probability rises at 0.35 eV and is about 0.007 when the collision energy is close to the barrier height of 0.43 eV, therefore showing a slight quantum tunneling effect. Such a behavior could be found for the probability on both CE-PES and this PES.[24] As for the excitation of the bending mode of the NH_2 radical, the probability is slightly larger than that of the ground state. This means that the excitation almost does not enhance the reactivity significantly. On the contrary, the excitation of NH_2 bending mode slightly hampers the reaction on the CE-PES. As for the excitation of the H_2 molecule, only a part of the excitation energy, about 0.2 eV out of 0.522 eV, is used to enhance reactivity. These values are the same as that obtained on the CE-PES. The

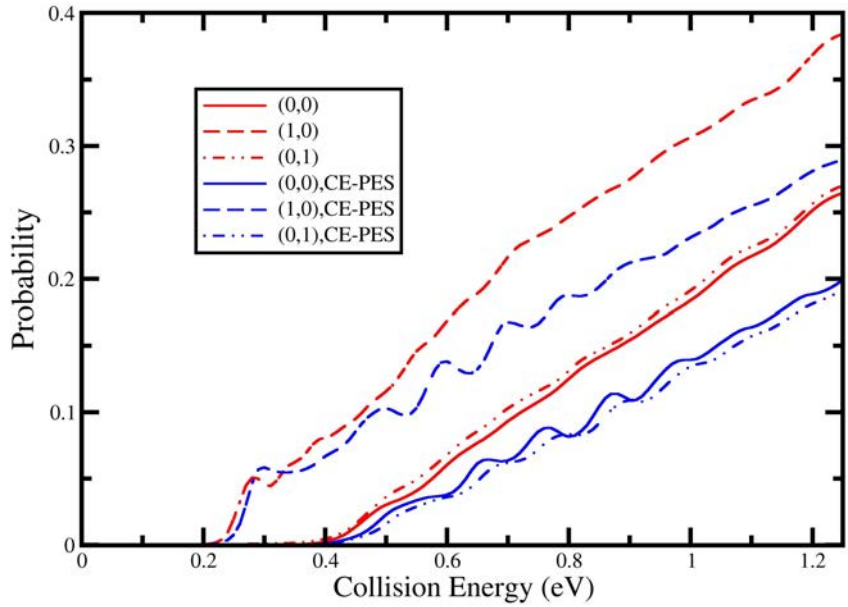

(a)

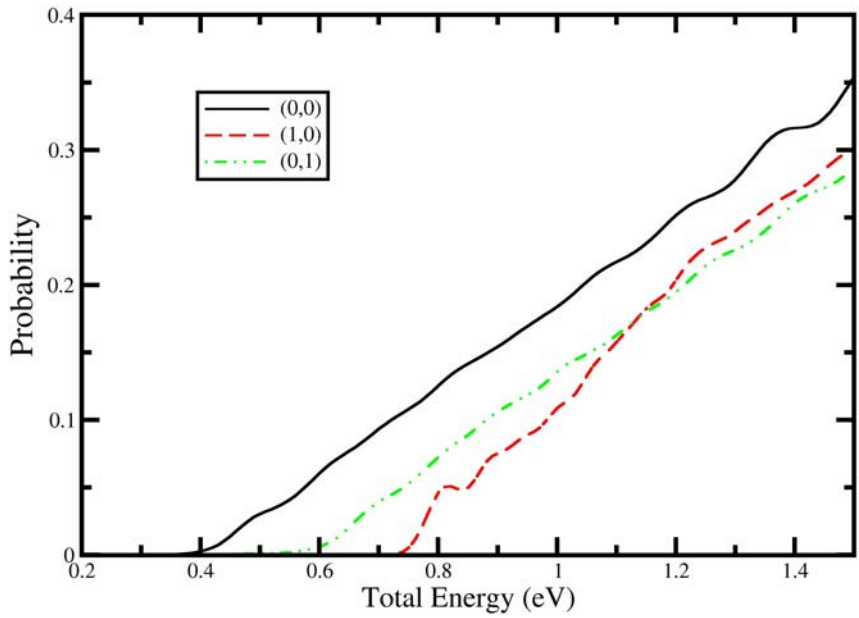

(b)

Fig. 4. (a) Total reaction probability for the $H_2(\nu_1) + NH_2(\nu_2)$ reaction as a function of translational energy. (b) Same as (a) except plotted as a function of total energy.

curves of probability with two PESs are very close and indicate that both PESs reflect important futures of this reaction. Also, one may note that the probability with the interpolated PES is overall slightly larger and smoother than that with CE-PES.

The ICS for a specific initial state is obtained by summing the total reaction probabilities over all the partial waves:

$$\sigma_{v_1 j_1 v_2 j_2}(E) = \frac{1}{(2j_1+1)(2j_2+1)} \frac{\pi}{2\mu E} \sum_{J_{\text{tot}}} (2J_{\text{tot}}+1) P^{J_{\text{tot}}}_{v_1 j_1 v_2 j_2}(E). \tag{12}$$

The exact close-coupling calculations for $J_{\text{tot}} > 0$ state are computationally expensive and the centrifugal-sudden (CS) approximation is employed in the calculations for $J_{\text{tot}} > 0$. The maximum value up to $J_{\text{tot}} = 50$ is used to converge the ICS calculation. Figures 5(a) and 5(b) show the ICSs for the three initial states as a function of collision energy and total energy, respectively. In accord with the reaction probabilities in Fig. 4, the reaction from the ground state contributes the most. However, for the total energy above 1.15 eV, the ICS for the reaction initially H_2 excited state is larger than that of the ground state, as shown in Fig. 5(b).

By comparing the breaking H_2 bond length in reactant/transition state (0.734 Å versus 0.887 Å) and the forming NH bond length in product/transition state (1.317 Å versus 1.015 Å), the $H_2 + NH_2$ reaction, this reaction is with an "early barrier". The calculated ICS could then be explained by Polanyi's rule[44]: the translational energy is more effective than the vibrational energy to enhance the reactivity.

The rate constants for the three initial states are calculated from the total reaction probabilities as:

$$r_i(T) = \left(\frac{2\pi}{(\mu kT)^3}\right)^{1/2} \sum_{J_{\text{tot}}} (2J_{\text{tot}}+1) \int_0^\infty \exp(-E_t/kT) P^{J_{\text{tot}}}_{v_1 j_1 v_2 j_2}(E_t) dE_t, \tag{13}$$

for $T = 200-2000$ K. The CS approximation and the J-shifting approximation were employed. The main contribution to the thermal rate constants comes from the ground state, in accord with the results of reaction probability calculations. The thermal rate constants calculated with the interpolated PES are generally overall larger than that with CE-PES, except at very low temperature. All available experimental values for this reaction collected in NIST Kinetic Database[45] are used to validate this PES. It is very interesting to note that the rate constants calculated with CE-PES[37] agree well with the measurement values at high temperature about 900−2000 K. While at intermediate temperature, the rate constants with the new interpolated PES are more accurate. This indicates the new PES is accurate at low energy but needs to be improved for higher energy region. However, one may note that these experimental rate constants show inconsistency as they are not very smooth as depicted in the Fig. 6.

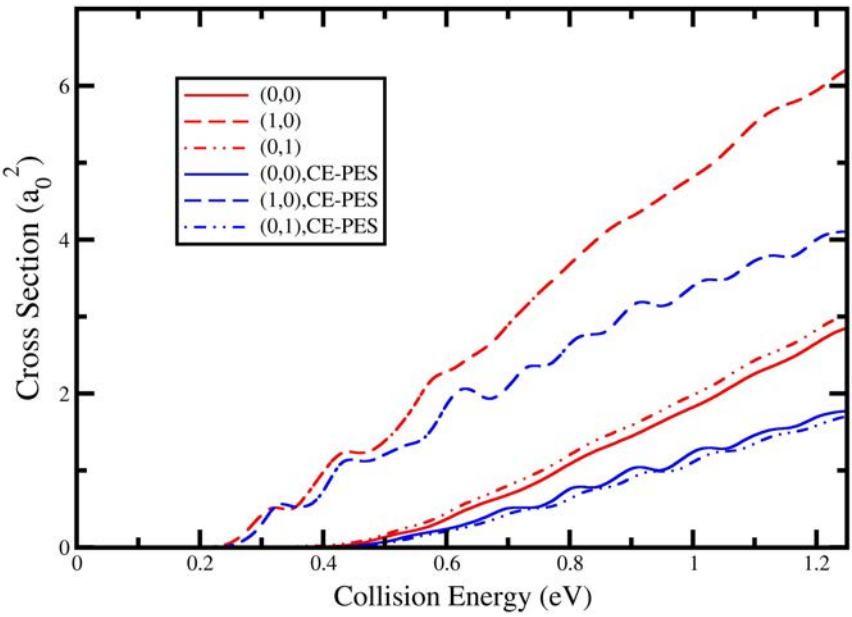

(a)

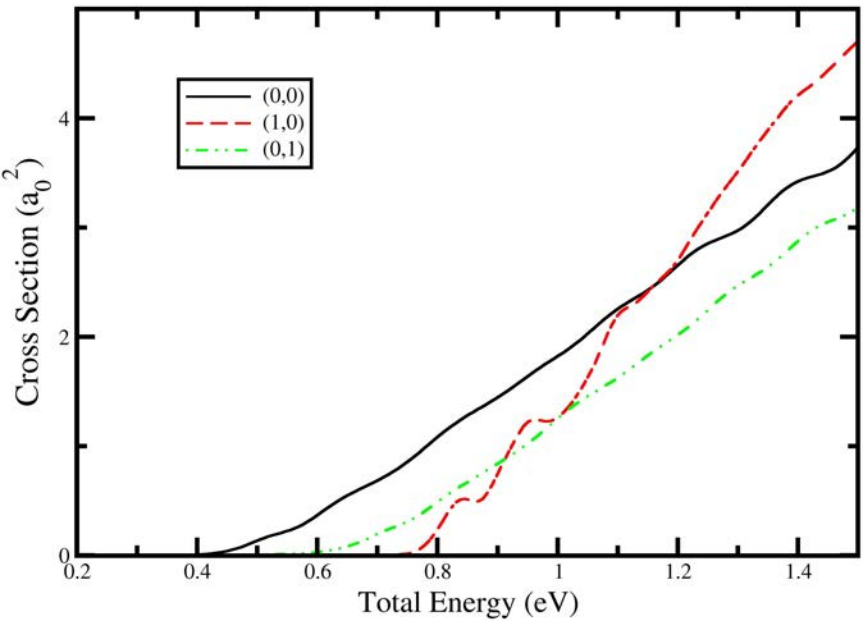

(b)

Fig. 5. ICSs for the $H_2(\nu_1) + NH_2(\nu_2)$ reaction as a function of translational energy. (b) Same as (a) except plotted as a function of total energy.

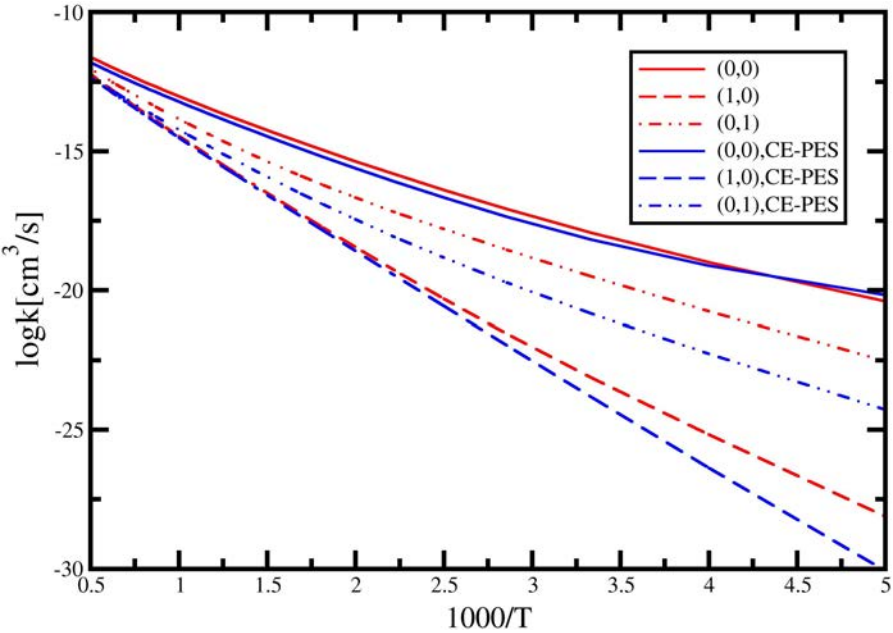

Fig. 6. Arrhenius plot of the initial state-selected rate constants.

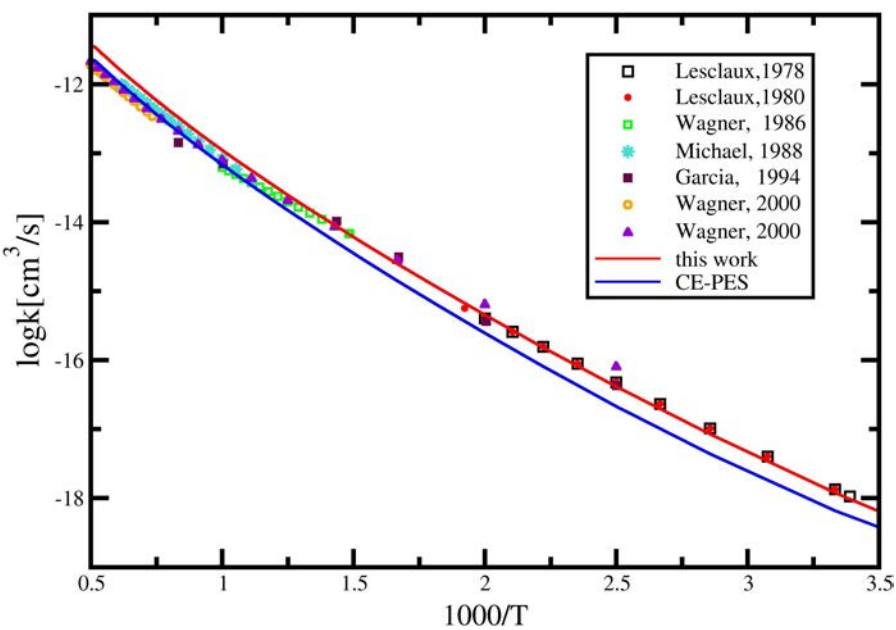

Fig. 7. Arrhenius plot of the experimental and calculated thermal rate constants. The experimental measurements are taken from NIST Kinetic Database.[45]

4. Conclusions

The time-dependent wave packet calculations have been carried out for $H_2 + NH_2$ reaction with a seven-dimensional model on a new interpolated *ab initio* PES. In the seven-dimensional model, NH_2 keeps C_{2v} symmetry and the NH bond lengths are fixed. The interpolated PES is constructed with Collins' modified Shepard interpolation scheme and contains 1967 data points. The *ab initio* calculations were carried out with UCCSD(T) method and with aug-cc-pVTZ basis set.

The reaction probabilities and the ICS for the reactants initially at, their ground states, when H_2 stretching and NH_2 bending mode are excited, are obtained and compared with the results calculated with Corchado and Espinosa-García's PES. The probabilities obtained with the new interpolated PES are about 30% larger than that with CE-PES. The conclusions drawn from calculations with two different PESs are generally similar: only part of the H_2 stretching excitation energy is deposited to promote the reaction while the excitation of NH_2 bending mode has no effect on enhancement of reactivity. And the translational energy is more efficient than vibration energy to accelerate this reaction with "early barrier", as predicted by Polanyi's rule.

The thermal rate constants calculated with the interpolated PES are generally overall larger than that with CE-PES. When comparing with the theoretical results with experimental measurements, the agreement is very good for the rate constants with CE-PES at high temperature between 900 K and 2000 K. While at intermediate temperature (from 293 K to 730 K), the rate constants calculated with the interpolated PES are almost coincident with the experimental values. These comparisons indicate that this interpolated PES is accurate for low energy region but needs to be improved at high energy region. The approximations employed in this work and the neglect of rotational and other vibrational excitations could be possibly the sources of the discrepancy between experiments and calculations.

Acknowledgments

This work is support by the National Natural Sciences of China (No. 21073229). The authors also thank Prof. M. A. Collins for providing the MC-PES.

References

1. Wang DY, *J Chem Phys* **124**:201105, 2006.
2. Yang XM, *Annu Rev Phys Chem* **58**:433, 2007.
3. Yang MH, *J Chem Phys* **129**:064315, 2008.
4. Schiffel G, Manthe U, *J Chem Phys* **133**:174124, 2010.
5. Wang FY, Lin JS, Liu KP, *Science* **331**:900, 2011.
6. Liu S, Xu X, Zhang DH, *J Chem Phys* **135**:141108, 2011.
7. Jankunas J, Zare RN, Bouakline F, Althorpe SC, Herraez-Aguilar D, Aoiz FJ, *Science* **336**:1687, 2012.
8. Liu KP, *Adv Chem Phys* **149**:1, 2012.

9. Zhang Z, Zhou Y, Zhang DH, Czako G, Bowman JM, *J Phys Chem Lett* **3**:3416, 2012.
10. Liu S, Xu X, Zhang DH, *J Chem Phys* **136**:144302, 2012.
11. Fu BN, Zhang DH, *J Phys Chem A* **116**:820, 2012.
12. Fu BN, Zhang DH, *J Chem Phys* **136**:194301, 2012.
13. Liu R, Yang M, Czako G, Bowman JM, Li J, Guo H, *J Phys Chem Lett* **3**:3776, 2012.
14. Liu R, Xiong HW, Yang MH, *J Chem Phys* **137**:174113, 2012.
15. Liu S, Chen J, Zhang ZJ, Zhang DH, *J Chem Phys* **138**:011101, 2013.
16. Bai LH, Zhang QG, Liu XG, *Acta Physica Sinica* **52**:2774, 2003.
17. Szichman H, Baer R, *J Chem Phys* **117**:7614, 2002.
18. Yang MH, Zhang DH, Lee SY, *J Chem Phys* **117**:9539, 2002.
19. Schiffel G, Manthe U, Nyman G, *J Phys Chem A* **114**:9617, 2010.
20. Chen J, Xu X, Zhang DH, *J Chem Phys* **138**:154301, 2013.
21. Czako G, Bowman JM, *J Chem Phys* **136**:044307, 2012.
22. Li Z, Xie CJ, Jiang B, Xie DQ, Liu L, Sun ZG, Zhang DH, Guo H, *J Chem Phys* **134**:134303, 2011.
23. Li L, Dong SL, *J Theor Comput Chem* **11**:1297, 2012.
24. Nie SS, Chu TS, *J Theor Comput Chem* **11**:1005, 2012.
25. Wang T, *J Theor Comput Chem* **11**:483, 2012.
26. Wei Q, *J Theor Comput Chem* **11**:811, 2012.
27. Yin SH, Guo MX, Zou JH, Xu XS, Che L, Li L, Gao H, *J Theor Comput Chem* **11**:791, 2012.
28. Yu YJ, Wang DH, Feng SX, Xia WZ, *J Theor Comput Chem* **11**:763, 2012.
29. Li J, Dawes R, Guo H, *J Chem Phys* **137**:094304, 2012.
30. Li J, Jiang B, Guo H, *Chem Sci* **4**:629, 2013.
31. Li J, Jiang B, Guo H, *J Am Chem Soc* **135**:982, 2013.
32. Li J, Jiang B, Guo H, *J Chem Phys* **138**:074309, 2013.
33. Yang X, Minton TK, Zhang DH, *Science* **336**:1650, 2012.
34. Yuan KJ, Cheng Y, Cheng L, Guo Q, Dai DX, Wang XY, Yang XM, Dixon RN, *Proc Nat Acad Sci USA* **105**:19148, 2008.
35. Zhang XQ, Cui Q, Zhang JZH, Han KL, *J Chem Phys* **126**:234304, 2007.
36. Yang MH, Corchado JC, *J Chem Phys* **126**:214312, 2007.
37. Yang MH, Corchado JC, *J Chem Phys* **127**:184308, 2007.
38. Corchado JC, EspinosaGarcia J, *J Chem Phys* **106**:4013, 1997.
39. Espinosa-Garcia J, Corchado JC, *J Phys Chem A* **114**:4455, 2010.
40. Moyano GE, Collins MA, *Theor Chem Acc* **113**:225, 2005.
41. Frisch MJ, Trucks GW, Schlegel HB *et al.*, *Gaussian 09, Inc., Wallingford, CT*, 2009.
42. Werner HJ, Knowles PJ, Knizia G *et al.*, *MOLPRO*, 2012.
43. Zhang DH, Zhang JZH, *J Chem Phys* **101**:1146, 1994.
44. Polanyi JC, *Acc Chem Res* **5**:161, 1972.
45. NIST, http://kinetics.nist.gov/kinetics/search.jsp.